12-29-2014

In Search of the X_2BO and X_2BS (X = H, F) Free Radicals: *Ab Initio* Studies of Their Spectroscopic Signatures

Dennis J. Clouthier
University of Kentucky, dclaser@uky.edu

In Search of the X_2BO and X_2BS (X = H, F) Free Radicals: *Ab Initio* Studies of Their Spectroscopic Signatures

Digital Object Identifier (DOI)
http://dx.doi.org/10.1063/1.4904290

Notes/Citation Information

Published in *The Journal of Chemical Physics*, v. 141, no. 24, article 244309, p. 244309-1 through 244309-9.

In search of the X_2BO and X_2BS (X = H, F) free radicals: *Ab initio* studies of their spectroscopic signatures

Dennis J. Clouthier[a)]
Department of Chemistry, University of Kentucky, Lexington, Kentucky 40506-0055, USA

(Received 22 October 2014; accepted 1 December 2014; published online 29 December 2014)

The F_2BO free radical is a known, although little studied, species but similar X_2BY (X = H, D, F; Y = O, S) molecules are largely unknown. High level *ab initio* methods have been used to predict the molecular structures, vibrational frequencies (in cm^{-1}), and relative energies of the ground and first two excited electronic states of these free radicals, as an aid to their eventual spectroscopic identification. The chosen theoretical methods and basis sets were tested on F_2BO and found to give good agreement with the known experimental quantities. In particular, complete basis set extrapolations of coupled-cluster single and doubles with perturbative triple excitations/aug-cc-pVXZ (X = 3, 4, 5) energies gave excellent electronic term values, due to small changes in geometry between states and the lack of significant multireference character in the wavefunctions. The radicals are found to have planar C_{2v} geometries in the $\tilde{X}^2B_2$ ground state, the low-lying $\tilde{A}^2B_1$ first excited state, and the higher $\tilde{B}^2A_1$ state. Some of these radicals have very small ground state dipole moments hindering microwave measurements. Infrared studies in matrices or in the gas phase may be possible although the fundamentals of H_2BO and H_2BS are quite weak. The most promising method of identifying these species in the gas phase appears to be absorption or laser-induced fluorescence spectroscopy through the allowed $\tilde{B}$-$\tilde{X}$ transitions which occur in the visible-near UV region of the electromagnetic spectrum. The *ab initio* results have been used to calculate the Franck-Condon profiles of the absorption and emission spectra, and the rotational structure of the $\tilde{B}$-$\tilde{X}0_0^0$ bands has been simulated. The calculated single vibronic level emission spectra provide a unique, readily recognizable fingerprint of each particular radical, facilitating the experimental identification of new X_2BY species in the gas phase. © *2014 AIP Publishing LLC.* [http://dx.doi.org/10.1063/1.4904290]

I. INTRODUCTION

Boron-containing free radicals are of interest in a variety of real world applications. For example, boron halides are widely used in the semiconductor industry[1–3] as feed gases in chemical vapor deposition, etching, and ion implantation processes, all of which can produce free radical intermediates. Boron compounds are also important in chemical hydrogen storage schemes, and their radicals may be intermediates in thermal regeneration cycles.[4] Boron derivatives have been characterized as key reagents in radical chemistry, and triethylborane is used as an effective low temperature initiator in radical reactions.[5] Boron has long been regarded as a good candidate for rocket fuel additives, due to its high energy density, and its incorporation results in complex high temperature chemistry involving boron radicals.[6] In these contexts, information on new boron radicals is both interesting and scientifically valuable.

Recently,[7] we have found that we can produce the F_2BO free radical, an unusual species previously observed[8,9] only once almost five decades ago, in a pulsed discharge jet and have characterized it by laser-induced fluorescence and emission spectroscopy. In anticipation of the possibility of "synthesizing" other such species in our discharge source, a series of high level *ab initio* calculations to predict the spectroscopic properties of the unknown X_2BO and X_2BS (X = H, D, F) free radicals have been undertaken, studies which are reported in the present work.

The best known of the subject radicals is F_2BO which was identified by Mathews and Innes[8] in investigations of the emission spectra obtained from discharges through BF_3/O_2 mixtures. The authors found two band systems, an extensive set of features near 5800 Å and a small group of bands with an intense 0-0 band at 4465 Å. Analysis of the spectra suggested that the carrier was either F_2BO or less likely F_2BO^+, either of which must be of C_{2v} symmetry in the combining states. Subsequent theoretical work[10,11] indicated that the emission band systems were due to the F_2BO free radical and could be assigned as $\tilde{B}^2A_1 \rightarrow \tilde{X}^2B_2$ (4465 Å) and $\tilde{B}^2A_1 \rightarrow \tilde{A}^2B_1$ (5800 Å). Most recently, the Clouthier group has reported[7] the LIF and emission spectra of jet-cooled $F_2{}^{11}BO$ and $F_2{}^{10}BO$ obtained by laser excitation of the bands near 4465 Å. Their combined experimental and *ab initio* results proved that the previously reported emission spectra were due to F_2BO[8,9] and substantially extended our knowledge of this free radical.

In 1976, Graham and Weltner reported detection of the H_2BO radical[12] among the products produced by vaporizing and trapping elemental boron in solid argon at 4-10 °K. It was identified by its ESR spectrum, which was very similar to that of the isoelectronic H_2CN free radical.[13] In more recent matrix infrared work, Jeong *et al.*,[14] cocondensed laser evaporated

a)Author to whom correspondence should be addressed. Electronic mail: dclaser@uky.edu

boron atoms with H_2O/Ar mixtures and observed infrared bands at 2573 and 2536 cm^{-1} (B–H stretches) and 1408 cm^{-1} (BO stretch), which they attributed to the HBOH molecule. No further experimental observations of H_2BO species have been reported, and the sulfur centered F_2BS and H_2BS free radicals have never been observed.

II. COMPUTATIONAL METHODS

The properties of the ground and first two excited doublet electronic states of the X_2BY (X = H, D, F; Y = O, S) free radicals have been calculated using a variety of methods with the Gaussian09 suite of programs.[15] Initially, density functional theory (DFT) with the Becke three parameter hybrid density functional[16] and the Lee, Yang, and Parr correlation functional[17] (B3LYP) and Dunning's correlation consistent basis sets augmented with diffuse functions[18] of triple-, quadruple-, and quintuple-zeta quality ([aug-]cc-pV(X)Z, X = T, Q, or 5) was employed. The basis sets for sulfur included a further tight *d* function [aug-cc-pV(X + d)Z] which facilitated convergence. Calculations including explicit electron correlation were conducted at the coupled-cluster single and doubles with perturbative triple excitations (CCSD(T)) level of theory with the same basis sets.

In order to correct for basis set truncation errors, complete basis set (CBS) extrapolations of the electronic energies of the various electronic states were done using the simple exponential function[19]

$$E_{(n)} = E_{CBS} + Ae^{-bn}, \quad (1)$$

where n is the basis set index with $n = 3$ for aug-cc-pVTZ, $n = 4$ for aug-cc-pVQZ, etc. The three parameters E_{CBS}, A, and b were exactly fit to the $n = 3$, 4, and 5 energies of a given electronic state to obtain the CBS extrapolated quantity.

Our CCSD(T)/aug-cc-pV5Z *ab initio* results were also used to perform Franck-Condon simulations of the absorption and single vibronic level (SVL) emission spectra of the various free radicals as an aid to their future detection by absorption, laser-induced fluorescence, and/or emission spectroscopy. The simulation program, originally developed by Yang *et al.*[20] and locally modified for the calculation of SVL emission spectra, requires input of the molecular structures, vibrational frequencies, and mass-weighted Cartesian displacement coordinates from the *ab initio* force fields of the two combining electronic states. Franck-Condon factors are then calculated in the harmonic approximation using the exact recursion relationships of Doktorov *et al.*[21] taking into account both normal coordinate displacement and Duschinsky rotation effects.

Finally, the equilibrium rotational constants and spin-rotation constants predicted by our B3LYP/aug-cc-pV5Z calculations have been used to simulate the absorption contours of the 0-0 bands of the free radicals under supersonic free jet expansion conditions. The very convenient graphical simulation program PGOPHER[22] was employed for this purpose.

III. RESULTS AND DISCUSSION

A. General considerations

Calculations using both the DFT and CCSD(T) methods with basis sets up to quintuple zeta quality all predicted the X_2BY radicals to be planar and of C_{2v} symmetry in the $\tilde{X}^2B_2$, $\tilde{A}^2B_1$, and $\tilde{B}^2A_1$ electronic states. The effect of spin contamination was minimal ($\langle S^2 \rangle$ differs from s(s + 1) by less than 1%). In order to evaluate the reliability of the single-reference coupled cluster wavefunctions and determine if they have appreciable multireference character, the T_1 diagnostic of Lee and coworkers[23] was computed. These calculations were done at the CCSD/aug-cc-pV5Z level of theory using our CCSD(T)/aug-cc-pV5Z optimized geometries. The highest value of $T_1 = 0.037$ was found for the ground state of H_2BO, with all the others below 0.027 and most below 0.02. Although closed-shell T_1 values larger than 0.02 are thought to signal significant multireference character, open-shell T_1 values are generally larger and the cutoff for suspect wavefunctions is less clear. Schaefer and co-workers[24] suggested that open-shell wavefunctions with T_1 values greater than about 0.045 should be considered suspect, and in this context, our results appear to be quite reliable.

The vibrational numbering convention used in this work is that of Herzberg[25] in which the vibrations are segregated by symmetry species and numbered starting with the highest frequency within each symmetry species. For ground state H_2BO, the vibrations are ω_1 (a_1) = symmetric B–H stretch, ω_2 (a_1) = B-O stretch, ω_3 (a_1) = HBH symmetric bend or scissoring, ω_4 (b_1) = out-of-plane bend, ω_5 (b_2) = B–H antisymmetric stretch, and ω_6 (b_2) = BH_2 antisymmetric bend or rocking. Although the numbering is unambiguous, the descriptions of the a_1 vibrations are only appropriate for H_2BO and are often either permuted or unclear due to extensive mixing of the internal coordinates for the other radicals.

Generally it was found that the geometries and vibrational frequencies, but not, of course, the energies, converged with quadruple zeta basis sets (aug-cc-pVQZ) and changed little with an increase in size to quintuple zeta (aug-cc-pV5Z). The DFT vibrational frequencies were usually slightly lower than the CCSD(T) values for a given basis set, with differences of the order of 20-30 cm^{-1} for the largest frequencies. The B3LYP/CBS T_0 values are found to be higher than the corresponding CCSD(T) values for the $\tilde{A}$ states but usually lower for the $\tilde{B}$ states.

B. Tests on F_2BO

In the series of radicals of interest in the present work, only the electronic spectrum of F_2BO is known, and the Clouthier group has recently explored its electronic spectroscopy in some detail.[7] Therefore, it served as a test molecule to prove the validity of the theoretical methods chosen to predict the properties of the unknown species. The experimentally determined properties of F_2BO compared to the present calculated values are summarized in Table I.

It is readily apparent that the CBS T_0 energies of the electronic states of F_2BO are calculated quite accurately, with errors of less than 100 cm^{-1} (<0.4%) with the CCSD(T)

TABLE I. Experimental and *ab initio* values [CCSD(T) values in brackets] (DFT values in parenthesis) of the vibrational frequencies and electronic energies of the boron isotopologues of F_2BO.

	$\tilde{X}^2B_2$		$\tilde{A}^2B_1$		$\tilde{B}^2A_1$	
Parameter[a]	$F_2{}^{11}BO$	$F_2{}^{10}BO$	$F_2{}^{11}BO$	$F_2{}^{10}BO$	$F_2{}^{11}BO$	$F_2{}^{10}BO$
T_0[b]	0	0	5218	5217	22 389	22 390
			[5156]	[5154]	[22421]	[22420]
			(5240)	(5238)	(21107)	(21105)
ω_1 (a_1)	1427	1475	1371	1415	...	...
(B-O stretch)[c]	[1449]	[1501]	[1382]	[1432]	[1294]	[1340]
	(1413)	(1464)	(1342)	(1391)	(1255)	(1300)
ω_2 (a_1)	876	875	857	856	...	...
(sym B-F stretch)[c]	[884]	[884]	[864]	[864]	[887]	[887]
	(877)	(877)	(857)	(857)	(883)	(883)
ω_3 (a_1)	463	466	492	493	481	481
(F_2 scissoring)	[461]	[463]	[491]	[493]	[483]	[485]
	(457)	(459)	(487)	(489)	(476)	(479)
ω_6 (b_2)[d]	386	387	455	453	497	495
(O rocking)	[387]	[388]	[454]	[456]	[499]	[501]
	(374)	(376)	(449)	(451)	(498)	(500)

[a]All quantities are in cm^{-1}.
[b]T_0 values from CBS T_e values plus aug-cc-pV5Z vibrational zero-point corrections. Vibrational frequencies are aug-cc-pV5Z values.
[c]Vibrational modes 1 and 2 both involve motion of the fluorine and oxygen atoms, so these descriptions are approximate.
[d]ω_6 experimental values are estimated as half the observed $2v_6$ intervals.

method. This level of agreement is fortuitously good and is unlikely to be the general case though the small changes in geometry, the predominantly single reference character of the wavefunctions, and the extrapolation to the CBS limit all aid in obtaining accurate predictions. The CCSD(T) and B3LYP harmonic vibrational frequencies generally bracket the observed vibrational fundamentals (where available), so they serve as a reasonable guide for making experimental assignments. The boron isotope shifts are more accurate and can generally be relied upon to within a few cm^{-1}, which is often within experimental accuracy for our typical emission spectra. In summary, the comparison of F_2BO experimental and theoretical electronic excitation energies and vibrational frequencies suggests that the theoretical methods employed should give estimates of the properties of unknown X_2BY species that are sufficiently reliable to make unambiguous experimental identifications.

C. X_2BY vs XBYX isomers

Although the X_2BY species of C_{2v} symmetry are the subject of this work, it was recognized that XBYX *cis* and *trans* isomers might also be stationary points on the potential energy surface. For HBOH, it was found that both geometric isomers with planar structures have minima with energies very close to the C_{2v} species. The transition states for the C_{2v}–*trans* and *trans*–*cis* isomerizations were also located with barriers of 32.6 and 9.9 kcal/mol [B3LYP/aug-cc-pV5Z], respectively. The energy level diagram in Fig. 1 shows the relative energies of the various species. At our highest of theory [CCSD(T)/aug-cc-pV5Z], the *trans* isomer was 0.2 kcal/mol lower than the C_{2v} radical, whereas the *cis* isomer was 1.7 kcal/mol above H_2BO. Clearly, all three species are likely to be made under the typical discharge jet conditions that we used to study F_2BO.[7]

The heavier H_2BS, F_2BO, and F_2BS species were studied at the B3LYP and CCSD(T) levels of theory with aug-cc-pVTZ basis sets; only the CCSD(T) relative energies are presented here. In contrast to HBOH, the planar *cis* and *trans* isomers of HBSH were calculated to be 23 and 22 kcal/mol, respectively,

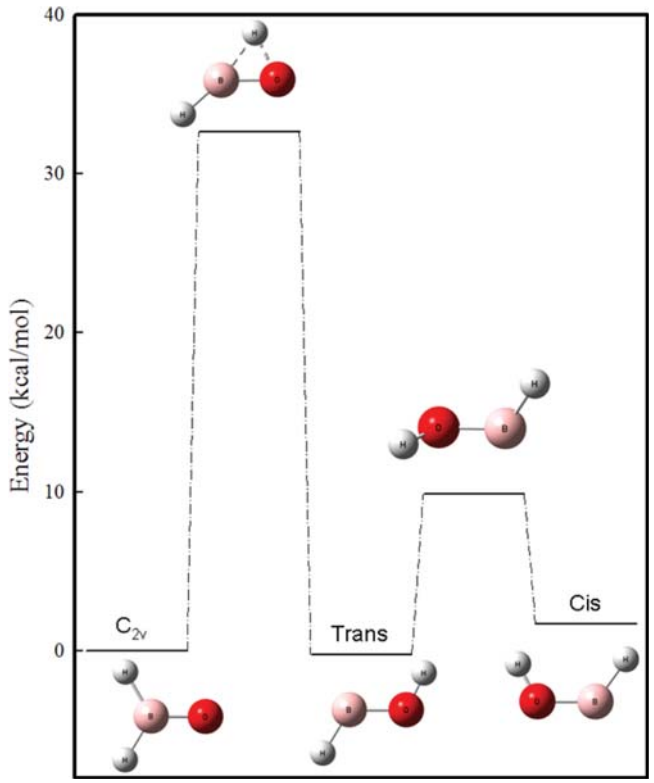

FIG. 1. A plot of the relative energies and structures of H_2BO, its *trans* and *cis* isomers and the transition states between the various isomers, obtained at the CCSD(T)/aug-cc-pV5Z level of theory.

TABLE II. *Ab initio* values of the structural and vibrational parameters [D_2BY or $X_2{}^{10}BY$ frequencies in brackets] for the ground states of the $X_2{}^{11}BY$ free radicals. (All with aug-cc-pV5Z basis sets.)

	$H_2{}^{11}BO$ [$D_2{}^{11}BO$]		$H_2{}^{11}BS$ [$D_2{}^{11}BO$]		$F_2{}^{11}BO$ [$F_2{}^{10}BO$]		$F_2{}^{11}BS$ [$F_2{}^{10}BS$]	
Parameter	CCSD(T)	DFT	CCSD(T)	DFT	CCSD(T)	DFT	CCSD(T)	DFT
r_{BY} (Å)	1.2919	1.2783	1.7321	1.7229	1.3639	1.3582	1.8019	1.8021
r_{BX} (Å)	1.2048	1.2077	1.1934	1.1928	1.3135	1.3175	1.3168	1.3199
θ_{XBY} (°)	118.95	120.30	119.00	119.74	119.29	119.34	120.56	120.59
Dipole moment (D)	1.0	1.6	0.33	0.26	0.05	0.11	0.83	0.74
ω_1 (cm^{-1})	2472 [1785]	2430 [1762]	2564 [1854]	2545 [1840]	1449 [1501]	1413 [1464]	1242 [1285]	1213 [1255]
ω_2 (cm^{-1})	1360 [1342]	1408 [1385]	1135 [930]	1107 [911]	884 [884]	877 [877]	683 [687]	672 [677]
ω_3 (cm^{-1})	1031 [750]	992 [719]	838 [724]	842 [724]	461 [463]	457 [459]	410 [410]	404 [404]
ω_4 (cm^{-1})	926 [744]	908 [732]	898 [710]	889 [704]	664 [691]	655 [682]	578 [602]	570 [594]
ω_5 (cm^{-1})	2537 [1887]	2466 [1831]	2653 [1982]	2618 [1954]	1447 [1499]	1413 [1464]	1398 [1447]	1361 [1409]
ω_6 (cm^{-1})	576 [461]	564 [452]	571 [436]	558 [427]	387 [388]	374 [376]	277 [279]	270 [272]

above the C_{2v} species, suggesting that the latter might be preferentially formed. For FBOF, only the planar *trans* isomer of C_S symmetry was found and it is some 125 kcal/mol above the global minimum. Similarly, planar *trans* FBSF was located 88 kcal/mol above F_2BS but no stable *cis* structure was predicted. These calculations show that the H_2BS, F_2BO, and F_2BS C_{2v} species are most likely to be the dominant products in any "synthesis".

D. Ground states of the X_2BY radicals

The ground state properties of the X_2BY radicals and their major isotopologues are summarized in Table II. The ground state electron configuration is ... $(a_1)^2$ $(b_1)^2$ $(b_2)^1$ yielding a $\tilde{X}^2B_2$ term symbol. The form of the molecular orbitals for H_2BO is shown in Fig. 2. The b_2 highest occupied molecular orbital (HOMO) is primarily an in-plane *p*-orbital on Y and is labeled as nonbonding (n_Y). The b_1 second highest occupied molecular orbital (SHOMO) is a π orbital between the B and Y atoms although the major contributor is the out-of-plane $2p_x$ orbital on the oxygen atom. Finally, the a_1 orbital is a σ orbital that is slightly bonding between B and Y, again with the major contribution from the $2p_z$ orbital on the oxygen atom. The form of the molecular orbitals is modified in the fluorine-containing species due to the participation of the fluorine 2*p* orbitals.

The ground state BO and BS bond lengths are H_2BO = 1.29 Å, F_2BO = 1.36 Å, H_2BS = 1.73 Å, and F_2BS = 1.80 Å. A comparison to the B=Y double bond lengths of HBO (1.201 Å),[26] HBS (1.598 Å),[27] FBO (1.207 Å),[28] and FBS (1.609 Å)[29] clearly shows that the X_2BY molecules, with BY bond lengths 0.09–0.19 Å longer, have a single bond between the boron atom and the terminal Y atom. In comparison to a molecule with a double bond such as formaldehyde, this is a result of the decreased bond order of the X_2BY σ + π bonds which are strongly polarized towards the terminal Y substituent. They compare more closely to the single bonds in H_2BOH (BO = 1.352 Å),[30] F_2BOH (BO = 1.346 Å),[31] and H_2BSH (BS = 1.778 *ab initio*).[32]

The BH bond lengths are in the range of 1.19–1.21 Å (H_2BS and H_2BO), whereas the BF bond lengths are in the

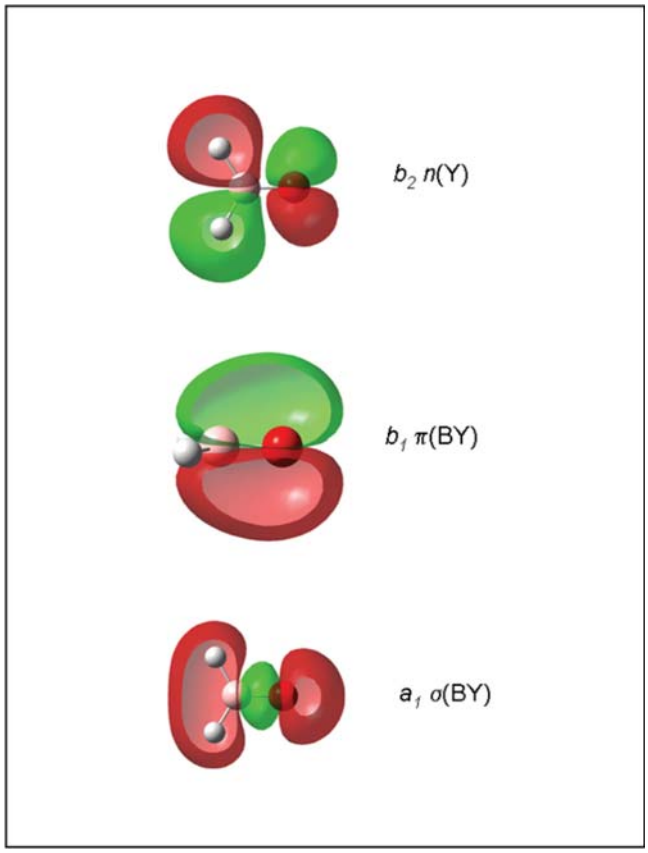

FIG. 2. Plots of the shapes of the three highest occupied molecular orbitals of H_2BO; HOMO (b_2), SHOMO (b_1), and THOMO (a_1).

TABLE III. *Ab initio* values of the structural, electronic, and vibrational parameters [D_2BY or $X_2{}^{10}BY$ values in brackets] for the $\tilde{A}^2B_1$ states of the $X_2{}^{11}BY$ free radicals. (All with aug-cc-pV5Z basis sets.)

	$H_2{}^{11}BO$ [$D_2{}^{11}BO$]		$H_2{}^{11}BS$ [$D_2{}^{11}BO$]		$F_2{}^{11}BO$ [$F_2{}^{10}BO$]		$F_2{}^{11}BS$ [$F_2{}^{10}BS$]	
Parameter	CCSD(T)	DFT	CCSD(T)	DFT	CCSD(T)	DFT	CCSD(T)	DFT
r_{BY} (Å)	1.4304	1.4301	1.8646	1.8668	1.4057	1.4012	1.8496	1.8535
r_{BX} (Å)	1.1930	1.1921	1.1885	1.1861	1.3113	1.3150	1.3126	1.3155
θ_{XBY} (°)	118.92	118.99	119.37	119.38	120.73	120.84	121.25	121.32
T_0 (cm^{-1})[a]	14 461 [14345]	15 710 [15578]	9120 [9060]	9922 [9854]	5156 [5154]	5240 [5238]	3464 [3463]	3581 [3580]
ω_1 (cm^{-1})	2586 [1871]	2566 [1855]	2606 [1883]	2598 [1876]	1382 [1432]	1342 [1391]	1236 [1277]	1204 [1243]
ω_2 (cm^{-1})	1302 [1141]	1289 [1126]	1230 [935]	1222 [925]	864 [864]	857 [857]	660 [666]	649 [654]
ω_3 (cm^{-1})	1089 [890]	1077 [883]	729 [679]	714 [668]	491 [493]	487 [489]	420 [420]	414 [414]
ω_4 (cm^{-1})	1023 [817]	1012 [808]	938 [740]	935 [737]	633 [659]	621 [647]	545 [568]	537 [559]
ω_5 (cm^{-1})	2679 [2011]	2655 [1993]	2706 [2030]	2694 [2021]	1448 [1501]	1408 [1460]	1412 [1462]	1376 [1425]
ω_6 (cm^{-1})	994 [776]	985 [770]	827 [626]	824 [624]	454 [456]	449 [451]	316 [318]	312 [314]

[a]T_0 values from CBS T_e values plus aug-cc-pV5Z vibrational zero-point corrections.

range of 1.31–1.32 Å (F_2BO and F_2BS). The former are slightly longer than the BH bonds in HBO (1.167 Å)[26] and HBS (1.170 Å),[27] consistent with the notion of overall weaker bonding in the radicals. The latter also follow the trend with longer BF bonds than in FBO (1.283 Å)[28] and FBS (1.276 Å)[29] but very similar to the 1.307 Å bond length[33] in BF_3. In all cases, the ground state X_2B bond angle is very close to 120°, indicating sp^2 hybridization on the central boron atom.

In each case, the Mulliken atomic spin density on the terminal Y atom is calculated to be essentially 1, indicating that the unpaired electron resides in an in-plane *p* orbital on the oxygen or sulfur atom. The spin-rotation constants $\boldsymbol{\varepsilon}_{aa}$, $\boldsymbol{\varepsilon}_{bb}$, and $\boldsymbol{\varepsilon}_{cc}$ all have negative signs in the ground state, with a particularly large $\boldsymbol{\varepsilon}_{aa} = -0.57$ cm^{-1} for H_2BS. The signs and relative values can be rationalized by considering that the dominant part of the spin-rotation interaction is given by the second-order perturbation theory expression[34,35] (considering only mixing of the ground state $\langle 0|$ with a single excited state $|n\rangle$, in this case the $\tilde{A}^2B_1$ state, which involves electron promotion from a lower orbital into the half-filled orbital)

$$\boldsymbol{\varepsilon}_{jj} = -4A_{SO}B_j \frac{|<0|L_b|n>|^2}{E(n)-E(0)}. \quad (2)$$

Here, $jj = aa$, bb, or cc; A_{SO} is the ground state molecular spin-orbit coupling constant; B_j is the rotational constant A, B, or C; $E(n)$ is the energy of the perturbing excited state; and $E(0)$ is the energy of the ground state. The integral in the numerator is usually approximated as 1 and A_{SO} may be crudely estimated from the atomic spin-orbit coupling constant[36] of the terminal oxygen ($\zeta = 151$ cm^{-1}) or sulfur ($\zeta = 382.4$ cm^{-1}) atom. Since in this case the denominator must be positive, it is evident that the ground state spin-rotation constants must have a negative sign. From Eq. (2), the major spin-rotation constants $\boldsymbol{\varepsilon}_{aa}$ are estimated [calculated *ab initio*] to be $H_2BO = -0.32$ [−0.07], $H_2BS = -1.31$ [−0.57], $F_2BO = -0.04$ [−0.00027], and $F_2BS = -0.13$ [−0.13] cm^{-1}. Clearly, the simple expression in Eq. (2), despite its many approximations, successfully reproduces the general trends predicted by the *ab initio* results, suggesting that the major contribution to ε''_{aa} is indeed due to the interaction with the low-lying $\tilde{A}^2B_1$ state.

The dipole moments of the radicals range from a low of ~0.1 D (F_2BO) to a high of 1.6 D (H_2BO) as given in Table II and are oriented, as required by symmetry, along the B–Y bond. The dipoles point with the negative end towards the Y atom except for F_2BS where the positive end is towards the sulfur atom. With the exception of F_2BO, which is a near-oblate asymmetric top, all the other radicals are near-prolate tops with $A > B \cong C$. The microwave spectra will consist of *a*-type $\Delta K_a = 0$ transitions, except in the F_2BO case, where I_b is along the C_2 symmetry axis and *b*-type transitions are expected. It is likely that the microwave spectra of H_2BO and F_2BS will be observable, but the pure rotational spectra of H_2BS and F_2BO will be very weak due to their very small dipole moments.

Matrix isolation techniques are expected to be the method by which the infrared spectra of these radicals will first be observed. For H_2BO, all the infrared bands are quite weak (maximum intensity ≈20 km/mol) with the strongest features predicted to be the ν_3 and ν_4 fundamentals between 900 and 1000 cm^{-1}. For H_2BS, all of the fundamentals are similarly weak with the strongest being the ν_5 fundamental near 2600 cm^{-1}. For F_2BO and F_2BS, the prospects are a bit better with strong ν_1 and ν_5 fundamentals in the 1400–1500 cm^{-1} and 1200–1350 cm^{-1} regions, respectively.

TABLE IV. *Ab initio* values of the structural, electronic, and vibrational parameters [D_2BY or $X_2{}^{10}BY$ values in brackets] for the $\tilde{B}^2A_1$ states of the $X_2{}^{11}BY$ free radicals. (All with aug-cc-pV5Z basis sets.)

	$H_2{}^{11}BO$ [$D_2{}^{11}BO$]		$H_2{}^{11}BS$ [$D_2{}^{11}BO$]		$F_2{}^{11}BO$ [$F_2{}^{10}BO$]		$F_2{}^{11}BS$ [$F_2{}^{10}BS$]	
Parameter	CCSD(T)	DFT	CCSD(T)	DFT	CCSD(T)	DFT	CCSD(T)	DFT
r_{BY} (Å)	1.3940	1.3828	1.8450	1.8414	1.3747	1.3654	1.8600	1.8571
r_{BX} (Å)	1.1947	1.1985	1.1849	1.1837	1.3077	1.3143	1.2986	1.3024
θ_{XBY} (°)	113.75	113.57	110.49	110.35	119.20	119.33	117.99	117.95
T_0 (cm^{-1})[a]	26878	26859	22348	22610	22421	21 107	23 175	22 397
	[26 781]	[26 758]	[22 308]	[22 565]	[22 420]	[21 105]	[23 174]	[22 396]
ω_1 (cm^{-1})	2513	2453	2579	2558	1294	1255	1136	1104
	[1799]	[1751]	[1841]	[1824]	[1340]	[1300]	[1167]	[1134]
ω_2 (cm^{-1})	1181	1195	1057	1065	887	883	617	610
	[1114]	[1129]	[823]	[825]	[887]	[883]	[625]	[619]
ω_3 (cm^{-1})	1085	1084	682	669	483	476	394	390
	[830]	[831]	[628]	[619]	[485]	[479]	[394]	[390]
ω_4 (cm^{-1})	1064	1060	951	952	690	679	579	571
	[843]	[841]	[743]	[743]	[718]	[706]	[603]	[595]
ω_5 (cm^{-1})	2650	2566	2762	2729	1477	1412	1509	1467
	[1995]	[1930]	[2085]	[2059]	[1532]	[1464]	[1564]	[1519]
ω_6 (cm^{-1})	976	972	759	744	499	498	319	319
	[760]	[759]	[568]	[557]	[501]	[500]	[320]	[321]

[a]T_0 values from CBS T_e values plus aug-cc-pV5Z vibrational zero-point corrections.

E. Excited electronic states of the X_2BY radicals

Promoting an electron from the doubly occupied SHOMO π orbital to the singly occupied n_Y HOMO yields the low-lying $\tilde{A}^2B_1$ state. The calculated properties of this state are summarized in Table III. The changes on electronic excitation differ between the hydrogen and fluorine-containing radicals: in H_2BO and H_2BS, the BY bond length elongates by 0.13 Å, suggesting that the π orbital has substantial bonding character, whereas in F_2BO and F_2BS, the bond elongation is only about 0.04 Å, indicating much weaker π bonding. The other geometric parameters are largely invariant although the F_2B bond angle *decreases* by ~3° (1.4°) in F_2BO (F_2BS).

The changes in the BY bond lengths are reflected in the BO (BS) stretching frequencies which decrease by 50 (100) cm^{-1} for H_2BO (H_2BS). The change is less clear for F_2BO (F_2BS) because both the ω_1 and ω_2 normal modes contain substantial BY stretching motion and both frequencies decrease on electronic excitation.

In all cases, the unpaired electron density in the π (b_1) orbital is predominantly on the terminal oxygen or sulfur, again indicating the strong polarization of the orbital towards the more electronegative (Pauling electronegativities: O = 3.4, S = 2.6, B = 2.0) atom. The major spin-rotation constants ε_{aa} are all positive and quite large, ranging from 0.21 cm^{-1} for H_2BO to 1.27 cm^{-1} for H_2BS, as would be expected by application of Eq. (2), since the denominator now has a negative sign.

The $\tilde{A}^2B_1$ states are quite low in energy, with the predicted excitation energies (T_0) decreasing monotonically from 14 461, 9120, 5156 to 3464 cm^{-1} going from H_2BO to F_2BS. The $\tilde{A}^2B_1 - \tilde{X}^2B_2$ electronic transitions are electronically forbidden but may borrow intensity from the allowed $\tilde{B}^2A_1 - \tilde{X}^2B_2$ system which occurs at higher energies. Such spectra may be observable for H_2BO and possibly H_2BS by LIF methods using red-sensitive detectors but the corresponding band systems of F_2BO and F_2BS occur in the mid-infrared and would require rather specialized techniques to study. Fortunately, the $\tilde{B}^2A_1 \rightarrow \tilde{A}^2B_1$ emission transitions are allowed and in the case of F_2BO, at least, are readily observable, providing direct experimental information on the $\tilde{A}$ state. Similar $\tilde{B} - \tilde{A}$ state transitions are expected for the other radicals, as discussed below.

Promotion of an electron from the slightly bonding σ third highest occupied molecular orbital (THOMO) to the nonbonding HOMO produces the B^2A_1 electronic excited state whose calculated properties are given in Table IV. In the hydrogenated radicals, there is a ≈0.1 Å increase in the B–Y bond length and a corresponding 10°–20° increase in the BH_2 bond angle, with little concomitant change in the B–H bond length. The fluorinated species undergo much smaller geometric changes on electronic excitation to the $\tilde{B}$ state, with F_2BO showing little variation and F_2BS exhibiting a 0.05 Å elongation of the BS bond and a 5° *increase* in the F_2B bond angle.

The $n \leftarrow \sigma$ electron promotion leaves the unpaired electron in the $\sigma(a_1)$ molecular orbital, and the Mulliken atomic spin densities indicate that the unpaired electron is more delocalized over the B and Y centers than it is in the $\tilde{X}$ or $\tilde{A}$ states, although roughly 75% of the spin density is on the oxygen in H_2BO and F_2BO, which decreases to about 55% in the sulfur radicals. The *ab initio* spin-rotation constants are uniformly small in the $\tilde{B}$ states (maximum value: $\varepsilon_{bb} = 0.044$ cm^{-1} for H_2BO), suggesting in the spirit of Eq. (2) that perturbations from states below and above lead to a near-cancellation of terms.

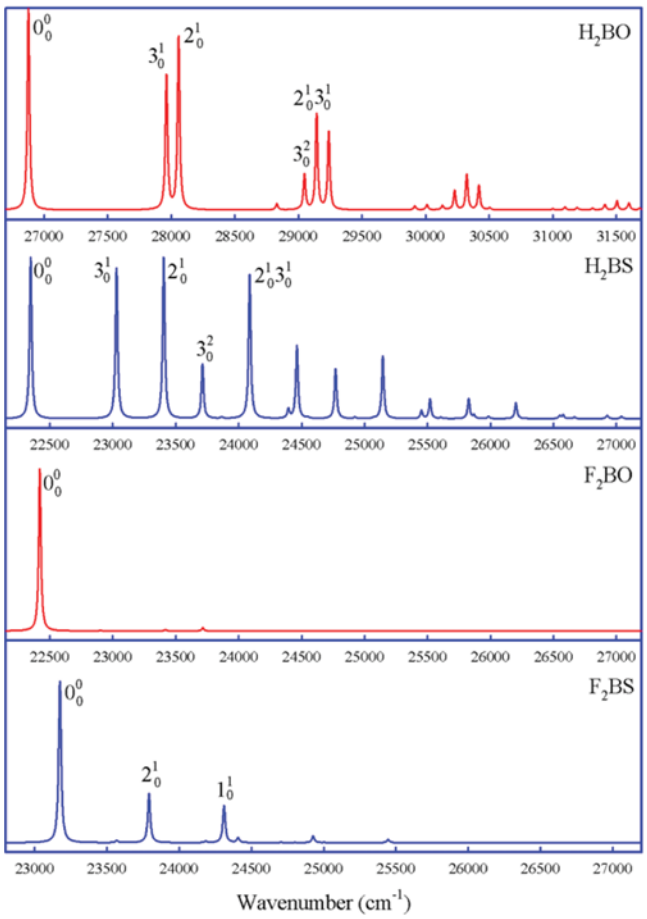

FIG. 3. Calculated Franck-Condon profiles of the $\tilde{B}$-$\tilde{X}$ cold band absorption spectra of the X_2BY radicals. The molecular geometries and vibrational frequencies are from CCSD(T)/aug-cc-pV5Z calculations with T_0 values taken from CBS extrapolations (Tables II and IV).

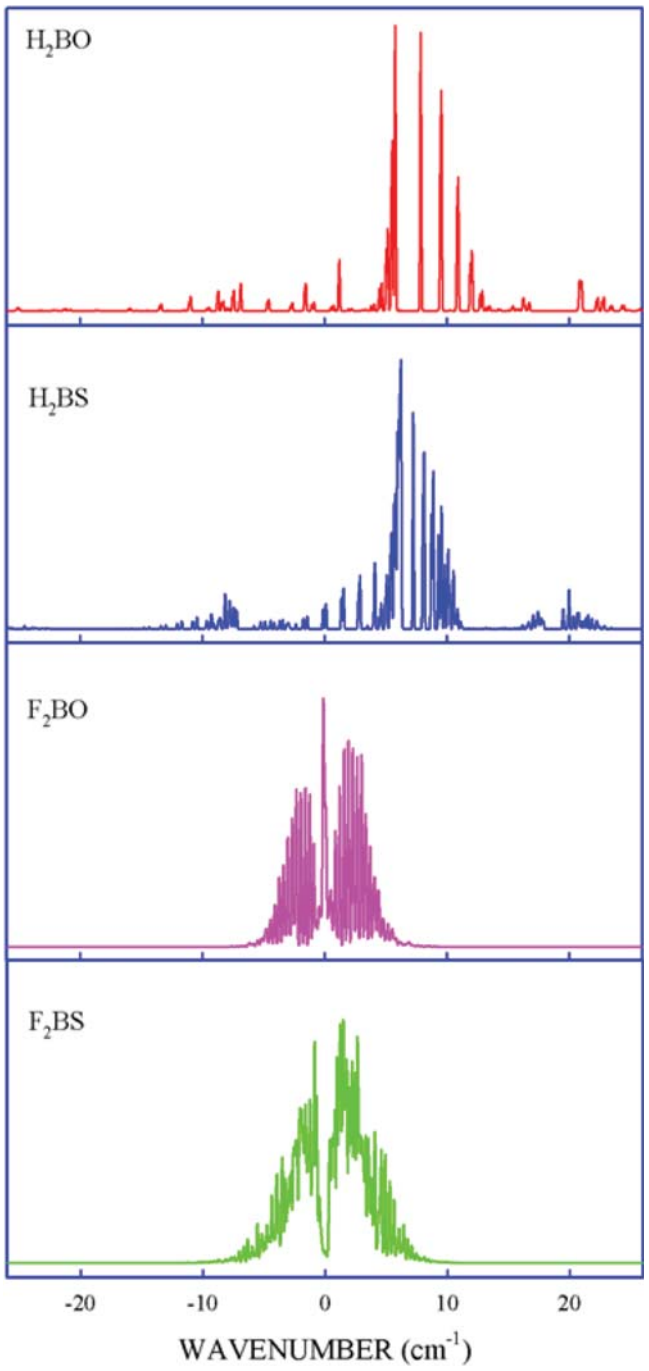

FIG. 4. Calculated rotational structure for the 0_0^0 bands of the X_2BY radicals at modest resolution (0.1 cm^{-1}) and a rotational temperature of 10 K. The rotational constants and spin-rotation constants were those obtained from B3LYP/aug-cc-pV5Z calculations.

Low level configuration interaction singles (CIS) calculations, at our CCSD(T)/aug-cc-pV5Z ground state geometries, indicate that the $\tilde{B}^2A_1 - \tilde{X}^2B_2$ systems are fairly weak with oscillator strengths ranging from 3×10^{-4} to 1.5×10^{-3}. Despite this limitation, LIF and emission spectra of F_2BO were readily observed, and all indications are that the spectra of the other radicals should also be accessible if they can be "synthesized" in reasonable yield. To this end, the $\tilde{B}$-$\tilde{X}$ absorption spectra and $\tilde{B}$ state 0-0 band single vibronic level emission spectra of the various radicals have been calculated, and the results are given in Figs. 3–5.

The Franck-Condon profiles of the $\tilde{B}$-$\tilde{X}$ cold band absorption spectra of the X_2BY radicals are illustrated in Fig. 3. Due to the significant geometry changes with electronic excitation, the spectra of H_2BO and H_2BS exhibit substantial Franck-Condon activity in the excited state BO (BS) stretching and X_2B symmetric bending (scissoring) modes. In agreement with the experiment, the calculated spectrum of F_2BO consists of a strong 0-0 band and little else, due to the similarities between the ground and excited state geometries. In F_2BS, there are a couple of additional bands but little vibronic activity in the spectrum. Due to the vibronic selection rules, activity in the totally symmetric modes is expected, and this is what is found with the exception of the 6_0^2 band which occurs weakly in some cases. The calculated spectra are for transitions from $v'' = 0$ although sequence bands (3_1^1, 4_1^1, 6_1^1, etc.) are observed in the F_2BO LIF spectra[7] and are likely to occur in the other radicals, depending on the extent of vibrational cooling in the experiment.

Fig. 4 shows the calculated rotational structure for 0_0^0 bands of the four radicals at modest resolution (0.1 cm^{-1}) and a rotational temperature of 10K. In each case, the ground and excited state rotational constants and spin-rotation constants

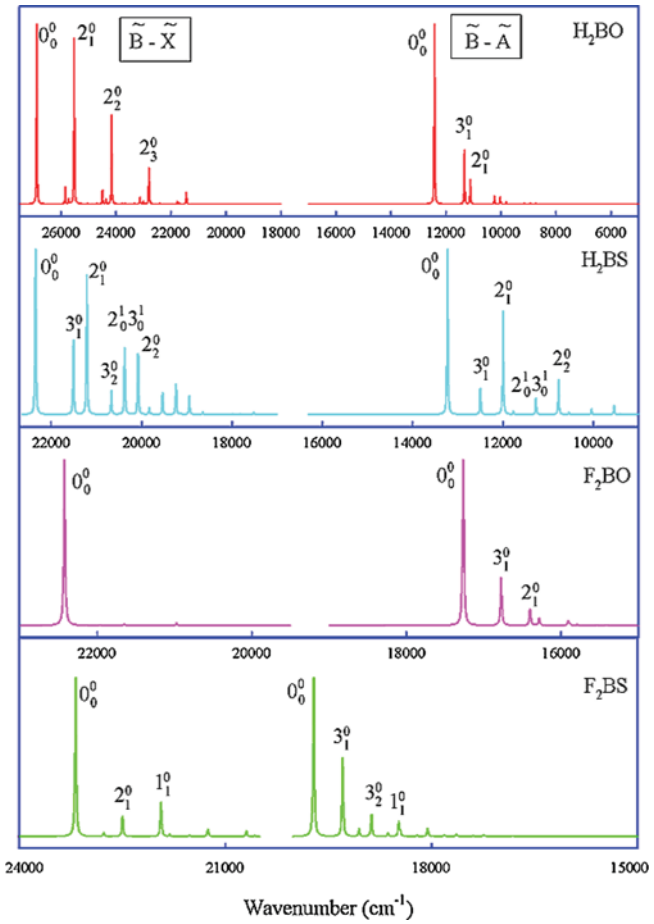

FIG. 5. Calculated Franck-Condon profiles of the $\tilde{B}$-$\tilde{X}$ and $\tilde{B}$-$\tilde{A}$ 0_0^0 band single vibronic level emission spectra of the X_2BY radicals. The molecular geometries and vibrational frequencies were from CCSD(T)/aug-cc-pV5Z calculations with T_0 values taken from CBS extrapolations (Tables II–IV). The break in the spectra indicates that the two emission spectra were calculated and normalized separately.

(ε_{aa}, ε_{bb}, and ε_{cc}) taken from our B3LYP calculations with quintuple zeta basis sets were used in the simulations. Substitution of the corresponding CCSD(T) rotational constants made little difference to the calculated spectra. In H_2BO, H_2BS, and F_2BS, the transition moment is along the in-plane intermediate moment of inertia and so the spectra exhibit near-prolate *b*-type rotational selection rules. In F_2BO, the radical is an oblate top with I_b along the C_2 axis and *a*-type bands occur in the spectrum. Due to the effect of nuclear statistical weights and Boltzmann factors, the jet-cooled spectra of H_2BO and H_2BS consist of a strong central $K_a' = 1 - K_a'' = 0$ subband with strong *R* and *Q* branches and weaker subbands originating from the less populated $K_a'' = 1$ rotational states. The spin splittings are readily apparent in the higher *N* members of the $^rR_0$ branch.

The 0-0 band spectrum of F_2BO exhibits a strong central *Q*-branch and a series of overlapping *P*- and *R*-branch features due to the operative $\Delta K_a = 0$ selection rules. The present spectrum, calculated with a larger basis set than previously, reproduces the observed splittings in *Q*-branch somewhat better than that reported in our experimental work on F_2BO.[7] The spectrum of F_2BS reverts back to *b*-type selection rules, yielding a central minimum and a complex mixture of overlapping subbands on either side.

Finally, Fig. 5 shows the calculated $\tilde{B}$ state 0-0 band single vibronic level emission spectra for the various radicals. In each case, two separate calculations were done, one of the Franck-Condon profile of $\tilde{B}^2A_1 - \tilde{X}^2B_2$ emission bands near the laser excitation frequency and a second of the profile of the $\tilde{B}^2A_1 - \tilde{A}^2B_1$ band system at much lower energies. In each case, the spectra were normalized to the strongest band, rotational structure was ignored, and there is no specific or implied information on the relative intensities of the two band systems. It is apparent that the $\tilde{B}$-$\tilde{X}$ emission spectra of H_2BO and H_2BO have fairly rich vibrational structure with activity in ν_2 and ν_3, while the $\tilde{B}$-$\tilde{A}$ band systems have less extensive progressions in the same modes. Mirroring the absorption spectrum, the 0-0 band dominates the $\tilde{B}$-$\tilde{X}$ emission spectrum of F_2BO, while the $\tilde{B}$-$\tilde{A}$ system includes weak 3_0^1 and 2_0^1 bands. Finally, the emission spectra of F_2BS exhibit activity in modes 1-3. It is important to emphasize that the emission spectra are very specific to each molecule and each provides a unique, readily recognizable fingerprint of the particular radical. Comparisons of these spectra to experimental data will provide the most conclusive low resolution evidence for the identification of new X_2BY species in the gas phase.

ACKNOWLEDGMENTS

The author is very grateful for the helpful discussions with Dr. Phil Sheridan of Canisius College. Thanks are also due to Robert Grimminger for discussions and some preliminary calculations. This research was supported by the National Science Foundation.

[1]S. J. Pearton, Mater. Res. Soc. Proc. **216**, 277 (1991).
[2]J. P. Langer and P. S. Dutta, J. Vac. Sci. Technol., B **21**, 1511 (2003).
[3]K. K. Baeck and R. J. Bartlett, J. Chem. Phys. **106**, 4604 (1997).
[4]D. J. Grant and D. A. Dixon, J. Phys. Chem. A **113**, 777 (2009).
[5]P. Renaud, A. Beauseigneur, A. Brecht-Forster, B. Becattini, V. Darmency, S. Kandhasamy, F. Montermini, C. Ollivier, P. Panchaud, D. Pozzi, E. M. Scanlan, A.-P. Schaffner, and V. Weber, Pure Appl. Chem. **79**, 223 (2007).
[6]S. H. Bauer, Chem. Rev. **96**, 1907 (1996).
[7]R. Grimminger, P. M. Sheridan, and D. J. Clouthier, J. Chem. Phys. **140**, 164302 (2014).
[8]C. W. Mathews and K. K. Innes, J. Mol. Spectrosc. **15**, 199 (1965).
[9]C. W. Mathews, J. Mol. spectrosc. **19**, 203 (1966).
[10]M. E. Jacox, J. Phys. Chem. Ref. Data **17**, 398 (1988).
[11]I. Baraille, C. Larrieu, A. Dargelos, and M. Chaillet, Chem. Phys. **282**, 9 (2002).
[12]W. R. M. Graham and W. Weltner, Jr., J. Chem. Phys. **65**, 1516 (1976).
[13]E. L. Cochran, F. J. Adrian, and V. A. Bowers, J. Chem. Phys. **36**, 1938 (1962).
[14]G. H. Jeong, R. Boucher, and K. J. Klabunde, J. Am. Chem. Soc. **112**, 3332 (1990).
[15]M. J. Frisch, G. W. Trucks, H. B. Schlegel *et al.*, GAUSSIAN 09, Revision A.02 Gaussian, Inc., Wallingford, CT, 2009.
[16]A. D. Becke, J. Chem. Phys. **98**, 5648 (1993).
[17]C. Lee, W. Yang, and R. G. Parr, Phys. Rev. B **37**, 785 (1988).
[18]T. H. Dunning, Jr., J. Chem. Phys. **90**, 1007 (1989).
[19]D. Feller, K. A. Peterson, and J. G. Hill, J. Chem. Phys. **135**, 044102 (2011).
[20]D. S. Yang, M. Z. Zgierski, A. Bérces, P. A. Hackett, P. N. Roy, A. Martinez, T. Carrington, Jr. Salahub, D. R. Fournier, R. Pang, and T. Chen, J. Chem. Phys. **105**, 10663 (1996).
[21]E. V. Doktorov, I. A. Malkin, and V. I. Man'ko, J. Mol. Spectrosc. **64**, 302 (1977).
[22]C. M. Western, PGOPHER, a program for simulating rotational structure, http://pgopher.chm.bris.ac.uk (University of Bristol, 2014).
[23]T. J. Lee and P. R. Taylor, Int. J. Quantum Chem., Quantum Chem. Symp. **36**(S23), 199 (1989).

[24]J. C. Rienstra-Kiracofe, W. D. Allen, and H. F. Schaefer III, J. Phys. Chem. A **104**, 9823 (2000).
[25]G. Herzberg, *Molecular Spectra and Molecular Structure II. Infrared and Raman Spectra of Polyatomic Molecules* (Van Nostrand, New York, 1945), p. 271.
[26]Y. Kawashima, Y. Endo, and E. Hirota, J. Mol. Spectrosc. **133**, 116 (1989).
[27]P. Turner and I. Mills, Mol. Phys. **46**, 161 (1982).
[28]Y. Kawashima, K. Kawaguchi, Y. Endo, and E. Hirota, J. Chem. Phys. **87**, 2006 (1989).
[29]L. Bizzocchi and C. D. Esposti, J. Chem. Phys. **115**, 7041 (2001).
[30]Y. Kawashima, H. Takeo, and C. Matsumura, J. Chem. Phys. **74**, 5430 (1981).
[31]J. Breidung, J. Demaison, J.-F. D'Eu, L. Margulès, D. Collet, E. B. Mkadmi, A. Perrin, and W. Thiel, J. Mol. Spectrosc. **228**, 7 (2004).
[32]D. J. Grant and D. A. Dixon, J. Phys. Chem. A **113**, 777 (2009).
[33]T. Masiello, A. Maki, and T. A. Blake, J. Mol. Spectrosc. **243**, 16 (2007).
[34]E. Hirota, J. Phys. Chem. **87**, 3375 (1983).
[35]R. N. Dixon, Mol. Phys. **10**, 1 (1965).
[36]H. Lefebvre-Brion and R. W. Field, *The Spectra and Dynamics of Diatomic Molecules* (Elsevier Academic Press, New York, 2004), p. 316.